SUPPLMENTARY METHODS

Total RNA isolation, cDNA preparation, and quantitative RT-PCR analysis

For the mRNA expression analyses, total RNA was extracted using TRIzol™ (Invitrogen) and purified using RNeasy mini columns (Qiagen). The M-MuLV first- strand cDNA synthesis kit (New England Biolabs) was used to generate cDNA according to the manufacturer's instructions. Quantitative RT-PCR was performed using the Power SYBR™ Green kit (Applied Biosystems) according to the manufacturer's instructions with ACTINB as an internal control. The primer sequences are provided in Table S2.

SDS-PAGE and Immunoblot analysis

Cell lysates were prepared using RIPA lysis buffer (Invitrogen) containing a Protease Inhibitor Cocktail (Roche) and a Phosphatase Inhibitor Cocktail (Sigma-Aldrich). Protein concentrations were determined using a BCA assay (Sigma-Aldrich). The proteins were then separated by SDS-polyacrylamide gel electrophoresis (PAGE) and transferred to polyvinylidene difluoride membranes. The membranes were blocked with 5% skim milk and hybridized overnight at 4°C with the primary antibodies listed in Table S2. The membranes were then incubated with the appropriate secondary HRP-conjugated antibody (GE Healthcare, UK) and the blots were developed using the SuperSignal West Pico Reagent (Pierce).

Autophagic vacuole staining

Autophagic vacuoles were detected by fluorescence microscopy using the Cyto-IDTM autophagy detection kit (Enzo Life Sciences). Briefly, the cells were collected by centrifugation and resuspended to a density of 1×10^6 cells/ml and washed twice with 1x assay buffer. The supernatants were carefully removed and the cells were resuspended in Microscopy Dual Detection Reagent solution and incubated for 30 min at 37°C in the dark. The cells were then washed with 1x assay buffer and resuspended in 500 µl of 1x assay buffer. DAPI was used to visualize the nucleus and the cells were analyzed by fluorescence microscopy. The fluorescence intensity was quantified using the ImageJ software.

MTT assay

For the MTT assay, 2×10^3 cells were plated in a 100 μl volume in 96-well plates. After 24 h, a range of concentrations of the indicated drugs were mixed in 100 μl of medium and added to the cells. On day 3 and 10 after treatment, the cell viability was evaluated by dissolving 20 μl of 5 mg/ml MTT solution in 1× PBS, adding the solution to each well, and incubating the cells for 1 h in a 37ºC incubator. After incubation, the MTT solution was gently removed and 100 μl of DMSO was added. The DMSO was mixed well by pipetting, and the absorbance was measured at 590 and 630 nm. An average was calculated for both readings, and the 630 nm measurement was subtracted from the 590 nm measurement. The relative growth rate was then plotted with respect to vehicle-treated control cells.

Apoptosis measurement using Annexin V-FITC staining

Apoptosis was analyzed by flow cytometry using the FITC Annexin V Apoptosis Detection Kit I (BD Pharmingen) per the manufacturer's protocol. Briefly, on day 3 and 10 after treatment with indicated drugs, the cells were washed twice with cold PBS and resuspended in 1x binding buffer at a concentration of 1 x 10^6 cells/ml. Next, 1 x 10^5 cells were incubated with FITC Annexin V for 15 min at RT in the dark. An additional 400 µl of binding buffer was then added to each sample and the samples were analyzed by flow cytometry within 1 h. Unstained cells were used as controls.

Site-directed mutagenesis

The pCMV-SPORT6-EZH2 plasmid was used as a template to generate $EZH2^{Y641F}$, $EZH2^{C663Y}$, $EZH2^{E720G}$, and $EZH2^{Y726F}$. The mutants were generated using the QuikChange XL Site-Directed Mutagenesis Kit (Agilent Technologies). The wild type and mutant *EZH2* sequences were PCR amplified, digested with BamH1 and Sal1, and cloned into the pBabe-puro vector (#1764; Addgene). All of the constructs were confirmed by sequencing. Primers used for site-directed mutagenesis are provided in Table S2.

Ingenuity Pathway Analysis

Gene expression profiles were analyzed using the Ingenuity Pathway Analysis software after exportation of the data from previously published GEO Datasets[15] (Accession# GSE40971). The top 250 altered genes were then submitted to Ingenuity Pathway Analysis to obtain a network based on the Ingenuity database.

Cell culture and plasmids

The SU-DHL-10 cells were purchased from the American Type Culture Collection (ATCC) and grown as recommended. The KARPAS-422 and WSU-DLCL-2 cells were purchased from Sigma-Aldrich and the Leibniz Institute DSMZ-German Collection of Microorganisms and Cell Cultures, respectively, and grown as recommended by the suppliers. The pBABE-puro cyclin D1 HA (#9050; Addgene), pBabe-puro HA PIK3CA H1047R (#12524; Addgene), pBABE-bleo IGF-1R (#11212; Addgene), and pBabe-Puro-MEK-DD (#15268; Addgene) were purchased from Addgene.

shRNAs and generation of retroviruses and lentiviruses and generation of stable lines

The *TNFSF10B, BAD, FOXO3A* shRNAs cloned in the pLKO.1 lentiviral expression vectors were obtained from Open Biosystems and are listed in Table S2. For retrovirus or lentivirus production, the constructs and viral packaging plasmids *Gag-Pol* and *VSV-G* or pSPAX2 and pMD2.G, respectively, were co-transfected into 293T cells using Effectene® (Qiagen) per the manufacturer's recommendations. The retroviral particles were prepared as previously described[20]. The virus was concentrated by incubation with the Lenti-X Concentrator (Clontech) as recommended by the supplier. The concentrated virus particles were used to infect SU-DHL-10, KARPAS-422 and WSU-DLCL-2 cells by spinfection and the cells were selected by growth on puromycin or zeocin 48 h after infection.

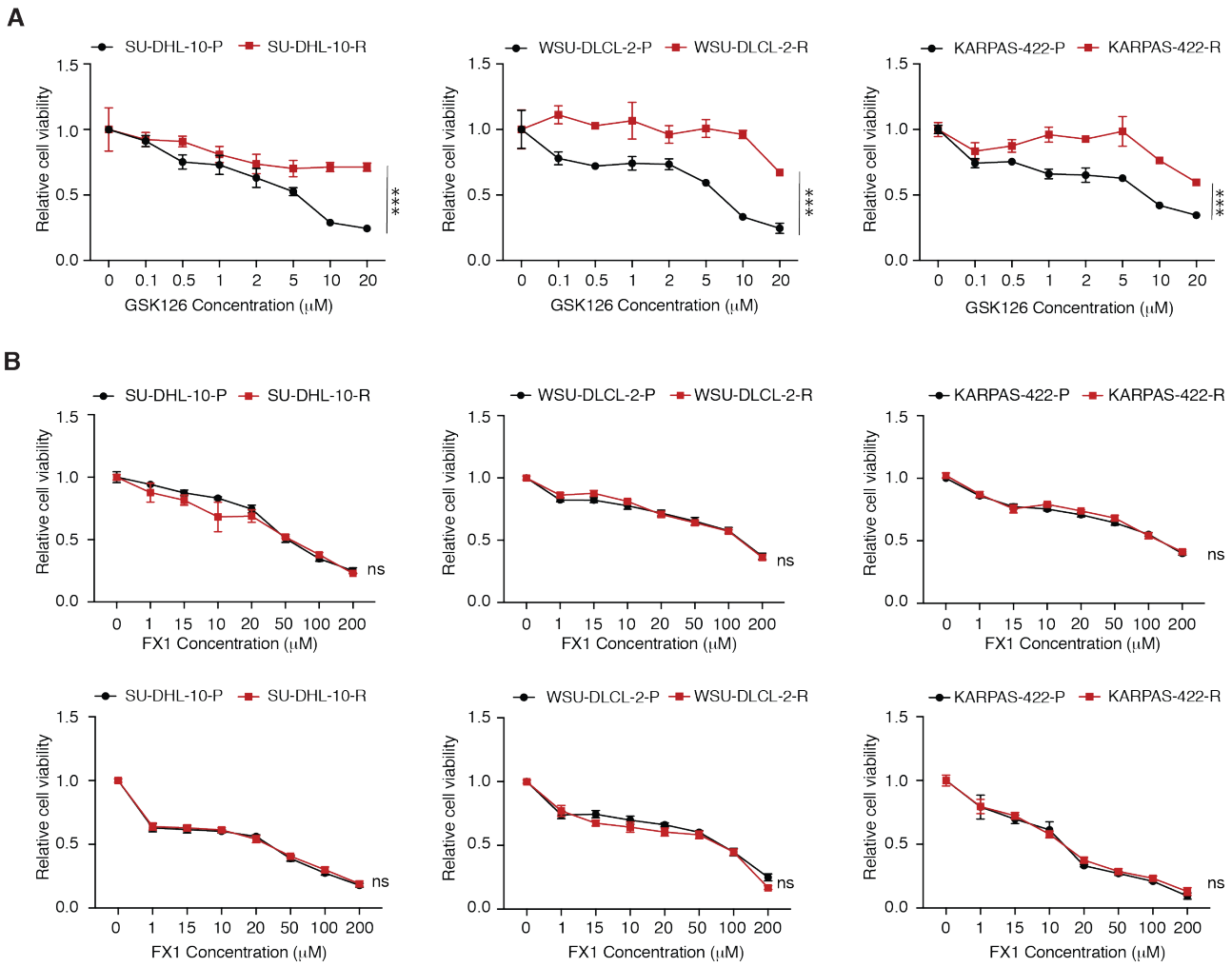

Figure S1. Characterization of a new *in vitro* model of acquired resistance to the EZH2 inhibitor GSK126. (A) The parental (P) and GSK126-resistant (R) DLBCL cell lines were treated with the EZH2 inhibitor GSK126 at the indicated concentrations and analyzed for cell viability 10 days after treatment using an MTT assay (B) The parental and GSK126-resistant DLBCL cell lines were treated with the BCL6 inhibitor FX1 at the indicated concentrations for 72 h (Top) and 10 days (Bottom) and analyzed for cell viability using an MTT assay. An area under the curve (AUC) was calculated to allow for the comparison between the two curves and the p-values were calculated using a t-test. Data are presented as mean ±SEM; ns=not significant, *** = $p<0.001$.

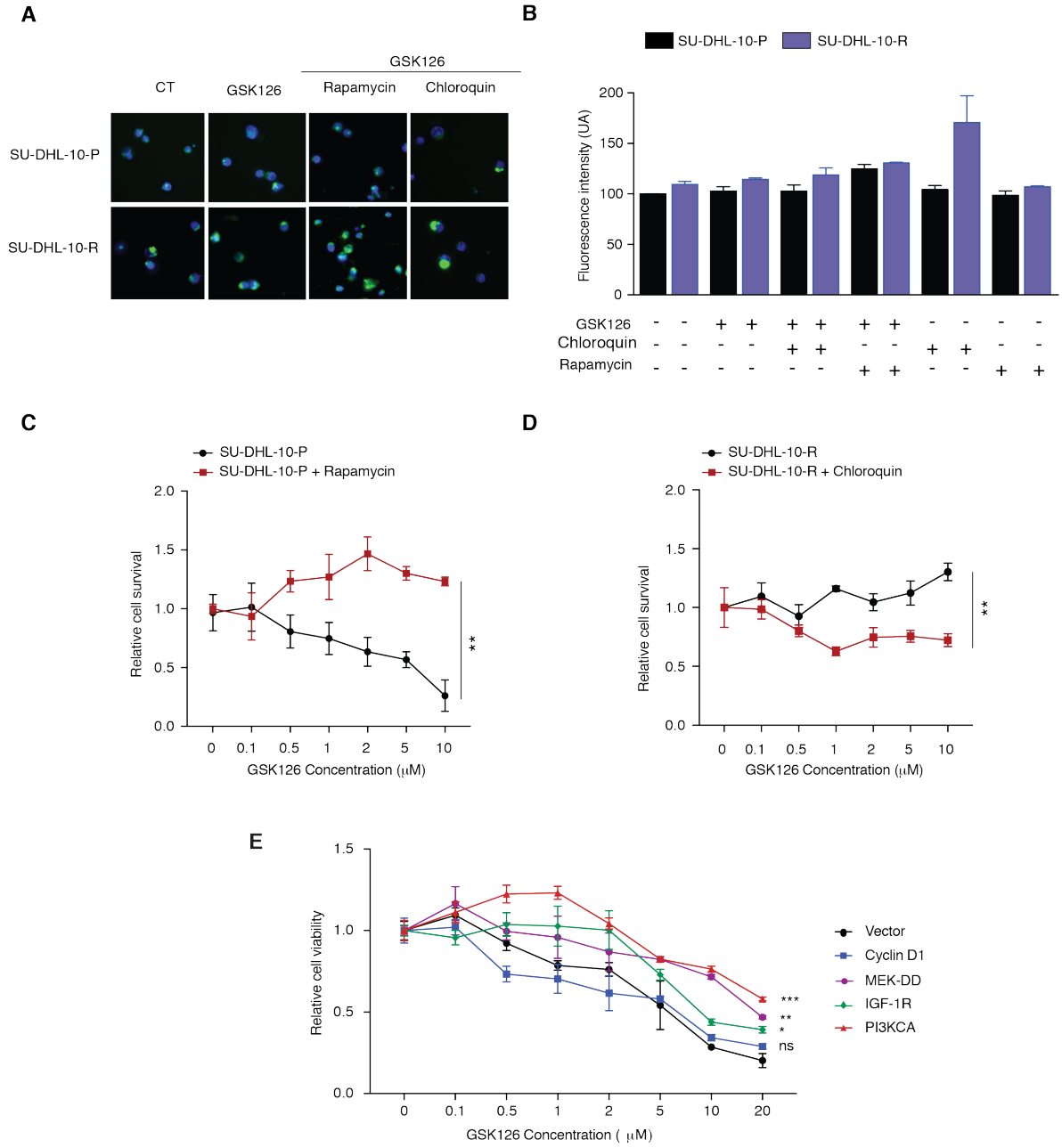

Figure S2. Autophagy does not play a role in conferring resistance to GSK126. (A) Autophagic vacuoles in SU-DHL-10 cells were stained with Cyto-ID™ following treatment with either GSK126 (1 μM) for 24 h alone or in combination with rapamycin (500 nM) for 12 h or chloroquin (10 μM) for 12 h. Nuclear DNA were stained with DAPI (blue). (B) The graph represents the quantification of fluorescence intensity (50 cells per condition, $n = 3$). (C) GSK126-sensitive SU-DHL-10 cells were treated with rapamycin (500 nM) and GSK126 at the indicated concentrations and analyzed by MTT after treatment for 72 h. The cell viability relative to untreated cells is shown. (D) GSK126-resistant SU-DHL-10 cells were treated with chloroquin (10 μM) and GSK126 at the indicated concentrations and analyzed by MTT after treatment for 72 h. The cell viability relative to untreated cells is shown. (E) SU-DHL-10 cells expressing the specified genes or an empty vector as a control (Vector) were analyzed for their sensitivity to GSK126 using an MTT assay after treatment with GSK126 at the indicated concentrations for 10 days. An area under the curve (AUC) was calculated to allow for the comparison between the two curves and the p-values were calculated using a t-test. Data are presented as mean ±SEM; ns=not significant, * = $p<0.05$, ** = $p<0.01$, *** = $p<0.001$.

A

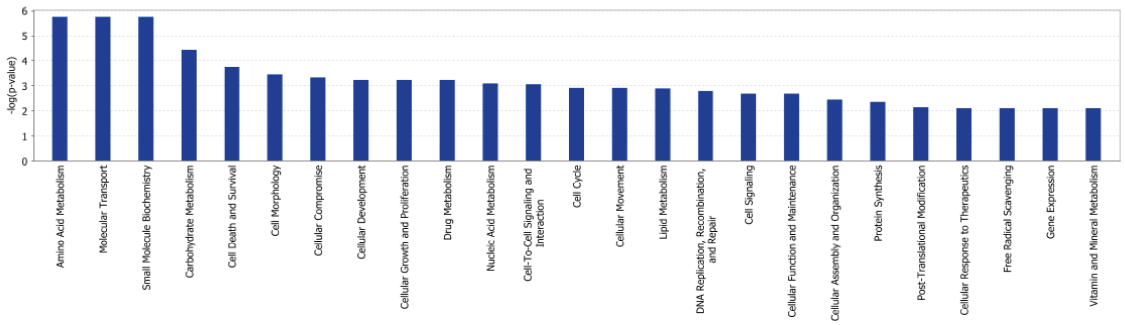

B

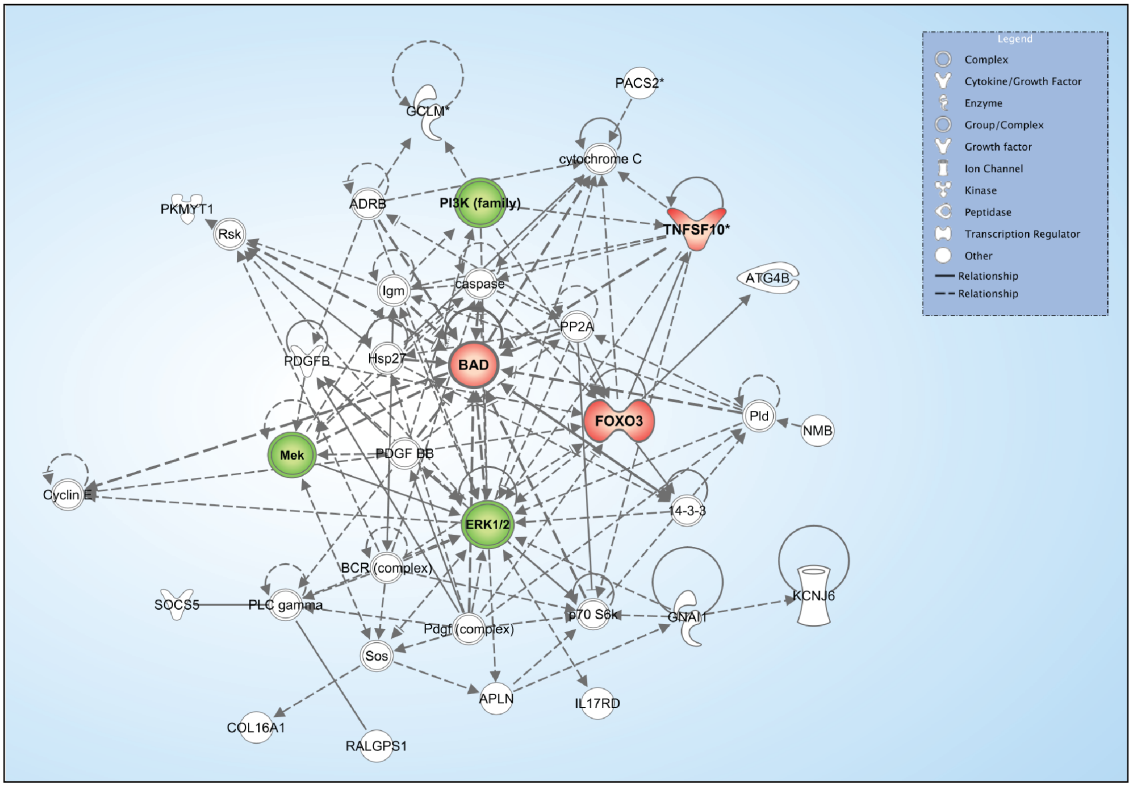

Figure S3. Identification of cell death related genes following GSK126 treatment. (A) Data were exported from previously published GEO Datasets (Accession# GSE:40971). The top 250 altered genes were submitted to Ingenuity Pathway Analysis and the genes were grouped by their functions previously reported in human and rodent studies. (B) All of the cell death and survival-related genes were mapped to obtain a network based on the Ingenuity database.

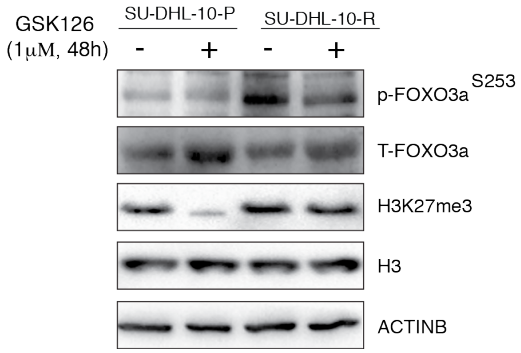

Figure S4. GSK126-resistant SU-DHL-10 cells display higher FOXO3A phosphorylation levels. SU-DHL-10-P or SU-DHL-10-R cells were treated with either DMSO or GSK126 (1 μM) for 48 h and analyzed for the expression of phospho-FOXO3A and H3K27me3 histone. Total-FOXO3A, Histone H3 and ACTINB were used as loading controls.

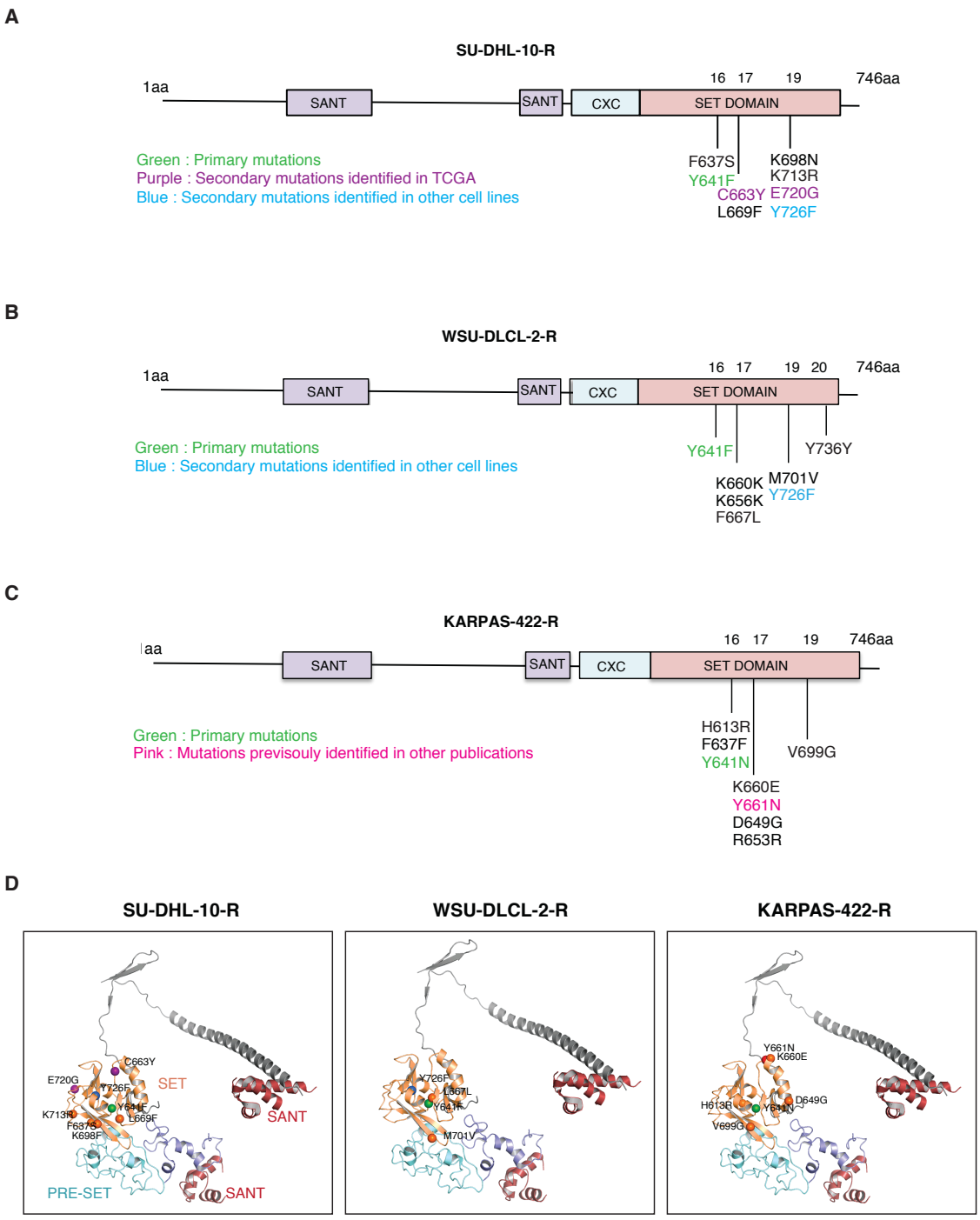

Figure S5. Identification of EZH2 mutations in GSK126-resistant DLBCL cells. (A-C) A schematic of the EZH2 protein structure is shown. Blue and Red correspond to the DNA-binding domain (CXC) and the SET catalytic domain, respectively. The mutations identified in SU-DHL-10-R (A) WSU-DLCL-2-R (B) and KARPAS-422-R cells (C) are shown. Primary mutations are indicated in green, mutations detected in multiple DLBCL cell lines are indicated in blue, and the mutations previously reported in other publications are labeled in pink. (D) The mutational landscape of all of the mutations in the SET domain of *EZH2* from GSK126-resistant DLBCL cell lines (SU-DHL-10-R, WSU-DLCL-2-R, and KARPAS-422-R) is shown and mapped onto crystal structure PDB ID: 5IJ7 [44]. The mutants are color coded as above and mutations that do not change the residue are not shown. Domains are indicated.

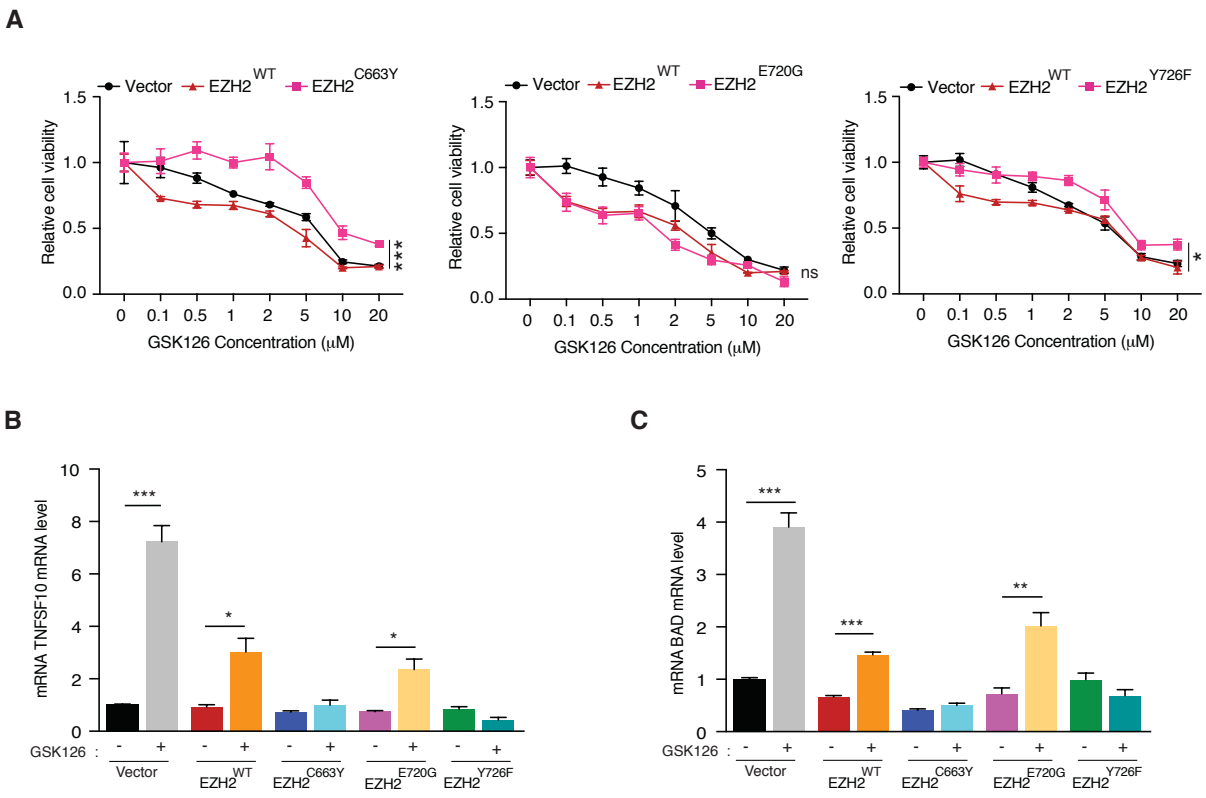

Figure S6. C663Y and Y726F confer resistance to GSK126 and repress GSK126-induced TNFSF10 and BAD expression in SU-DHL-10 cells. (A) SU-DHL-10 cells overexpressing either $EZH2^{WT}$, $EZH2^{C663Y}$, $EZH2^{E720G}$, $EZH2^{Y726F}$, or empty vector were treated with the specified concentrations of GSK126 for 10 days and assayed for cell viability using an MTT assay. The cell viability compared to untreated cells is shown. (B-C) *TNFSF10* and *BAD* mRNA expression in SU-DHL-10 cells overexpressing $EZH2^{WT}$, $EZH2^{C663Y}$, $EZH2^{E720G}$, $EZH2^{Y726F}$, or empty vector following treatment with GSK126 (1 μM) for 48 h. The *p*-values were calculated using a t-test. Data are presented as mean ±SEM; ns=not significant, * = $p<0.05$, ** = $p<0.01$, and *** = $p<0.001$.

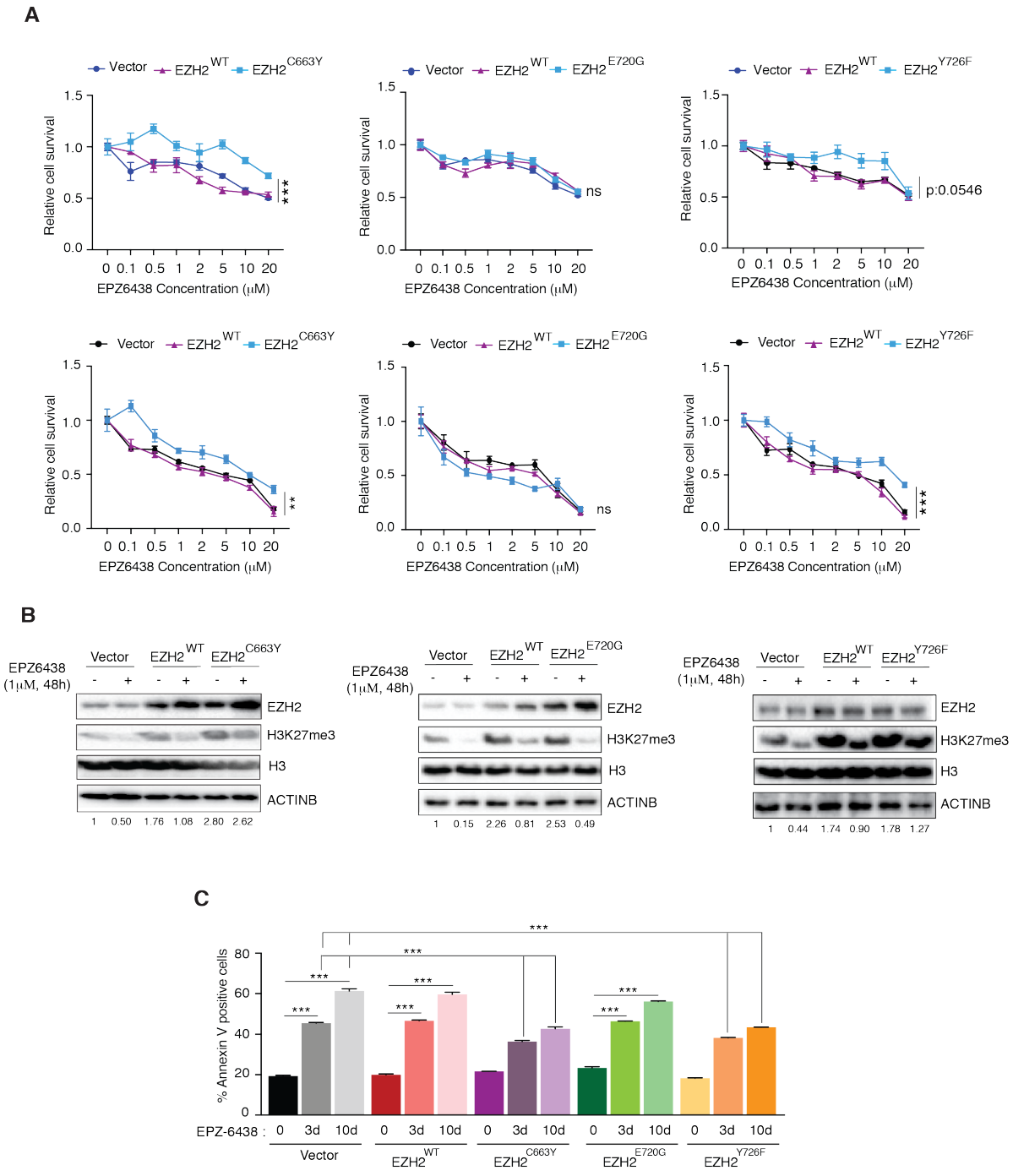

Figure S7. The EZH2^{C663Y} and EZH2^{Y726F} mutants confer resistance to EPZ-6438. (A) SU-DHL-10 cells overexpressing EZH2^{WT}, EZH2^{C663Y}, EZH2^{E720G}, EZH2^{Y726F}, or empty vector were treated with the specified concentrations of EPZ-6438 for 72 h (Top) or 10 days (Bottom) and assayed for cell viability by MTT. The cell viability relative to untreated cells is shown. (B) SU-DHL-10 cells overexpressing EZH2^{WT}, EZH2^{C663Y}, EZH2^{E720G}, EZH2^{Y726F}, or empty vector were treated with EPZ-6438 (1 μM) for 48 h and analyzed for EZH2 and H3K27me3 by immunoblotting. Histone H3 and ACTINB were used as loading controls. (C) SU-DHL-10 cells overexpressing either EZH2^{WT}, EZH2^{C663Y}, EZH2^{E720G}, EZH2^{Y726F}, or an empty vector were treated with EPZ-6438 (5 μM) for 3 or 10 days and apoptosis was analyzed by annexin V-FITC staining. An area under the curve (AUC) was calculated to allow for the comparison between the two curves and the p-values were calculated using a t-test. Data are presented as mean ±SEM; ns=not significant, ** = p<0.01, and *** = p<0.001.

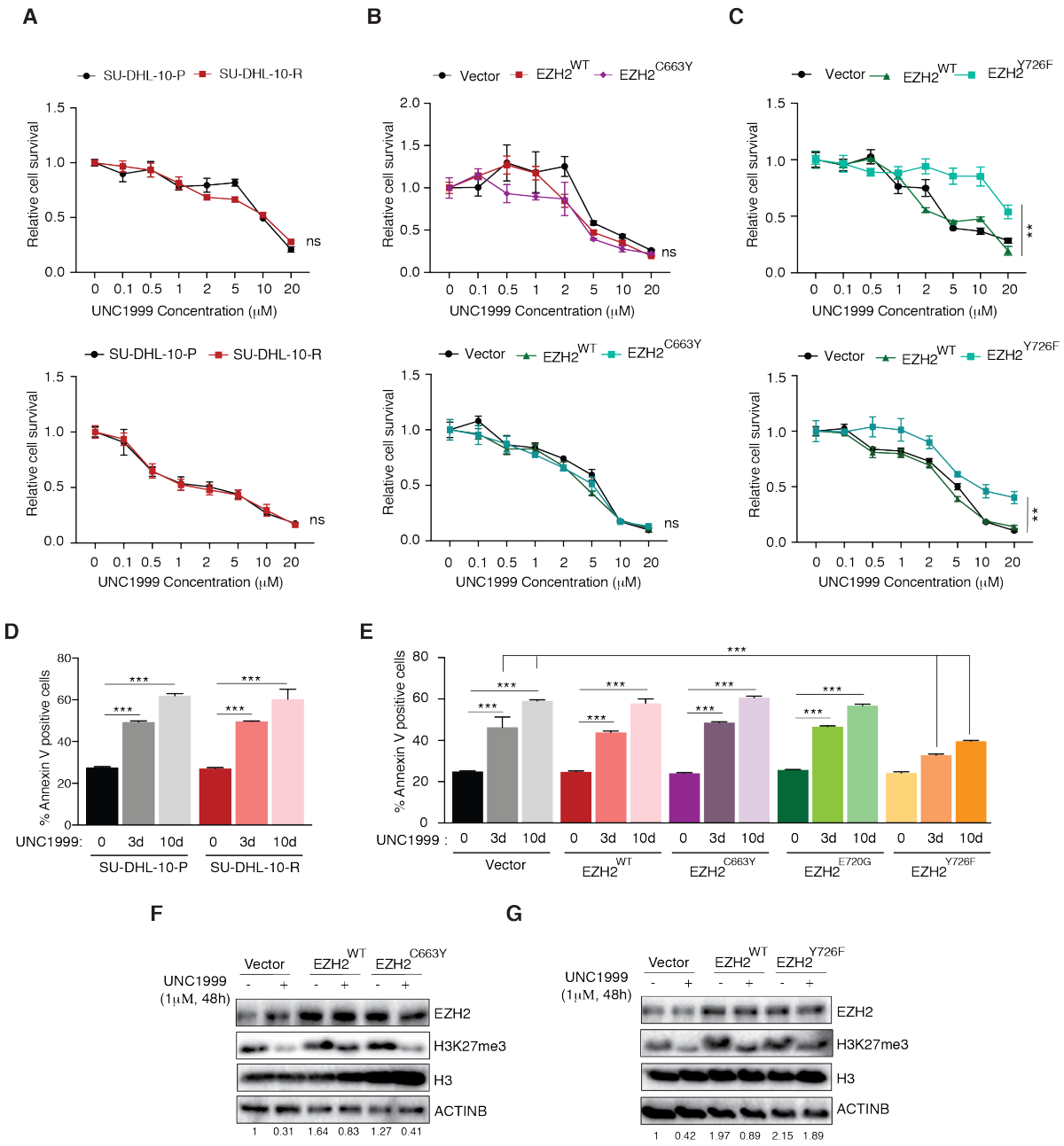

Figure S8. The EZH2^{C663Y} mutation does not confer resistance to the EZH2 inhibitor UNC1999. (A) Parental and GSK126-resistant SU-DHL-10 cells (SU-DHL-10-P and SU-DHL-10-R) were treated with the indicated concentration of UNC1999 for 3 days (Top) or 10 days (Bottom) and assayed for cell viability by MTT. (B-C). SU-DHL-10 cells stably expressing EZH2^{WT}, EZH2^{C663Y}, EZH2^{Y726F}, or empty vector were treated with the indicated concentrations of UNC1999 3 days (Top) or 10 days (Bottom) and assayed for cell viability by MTT. (D) Parental and GSK126-resistant SU-DHL-10 cells (SU-DHL-10-P and SU-DHL-10-R) were treated with UNC1999 (5 μM) for 3 or 10 days and apoptosis was analyzed by annexin V-FITC staining. (E) SU-DHL-10 cells overexpressing either EZH2^{WT}, EZH2^{C663Y}, EZH2^{E720G}, EZH2^{Y726F}, or an empty vector were treated with UNC1999 (5 μM) for 3 or 10 days and apoptosis was analyzed by annexin V-FITC staining. (F-G) SU-DHL-10 cells expressing either EZH2^{WT}, EZH2^{C663Y}, EZH2^{Y726F}, or empty vector were treated with UNC1999 (1 μM) for 48 h and analyzed for EZH2 and H3K27me3 by immunoblotting. Histone H3 and ACTINB were used as loading controls. An area under the curve (AUC) was calculated to allow for the comparison between the two curves and the p-values were calculated using a t-test. Data are presented as mean ±SEM; ns=not significant, ** = p<0.01, and *** = p<0.001.

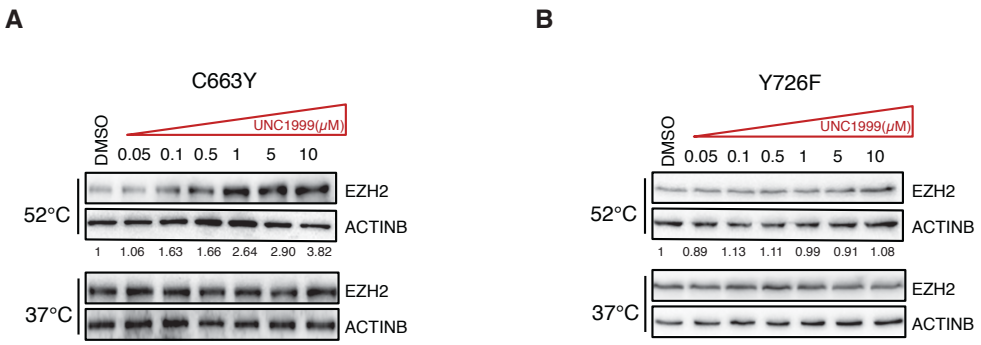

Figure S9. EZH2^{Y726F} alters UNC1999 binding to EZH2, whereas EZH2^{C663Y} does not. (A-B) A cellular shift thermal assay was performed in SU-DHL-10 cells stably expressing EZH2^{C663Y} (A) or EZH2^{Y726F} (B) and treated with incremental doses of the EZH2 inhibitor UNC1999 for 4 h at 52°C. Samples maintained at 37°C served as the EZH2 thermo-stability control. The samples were analyzed for EZH2 and ACTINB by immunoblotting.

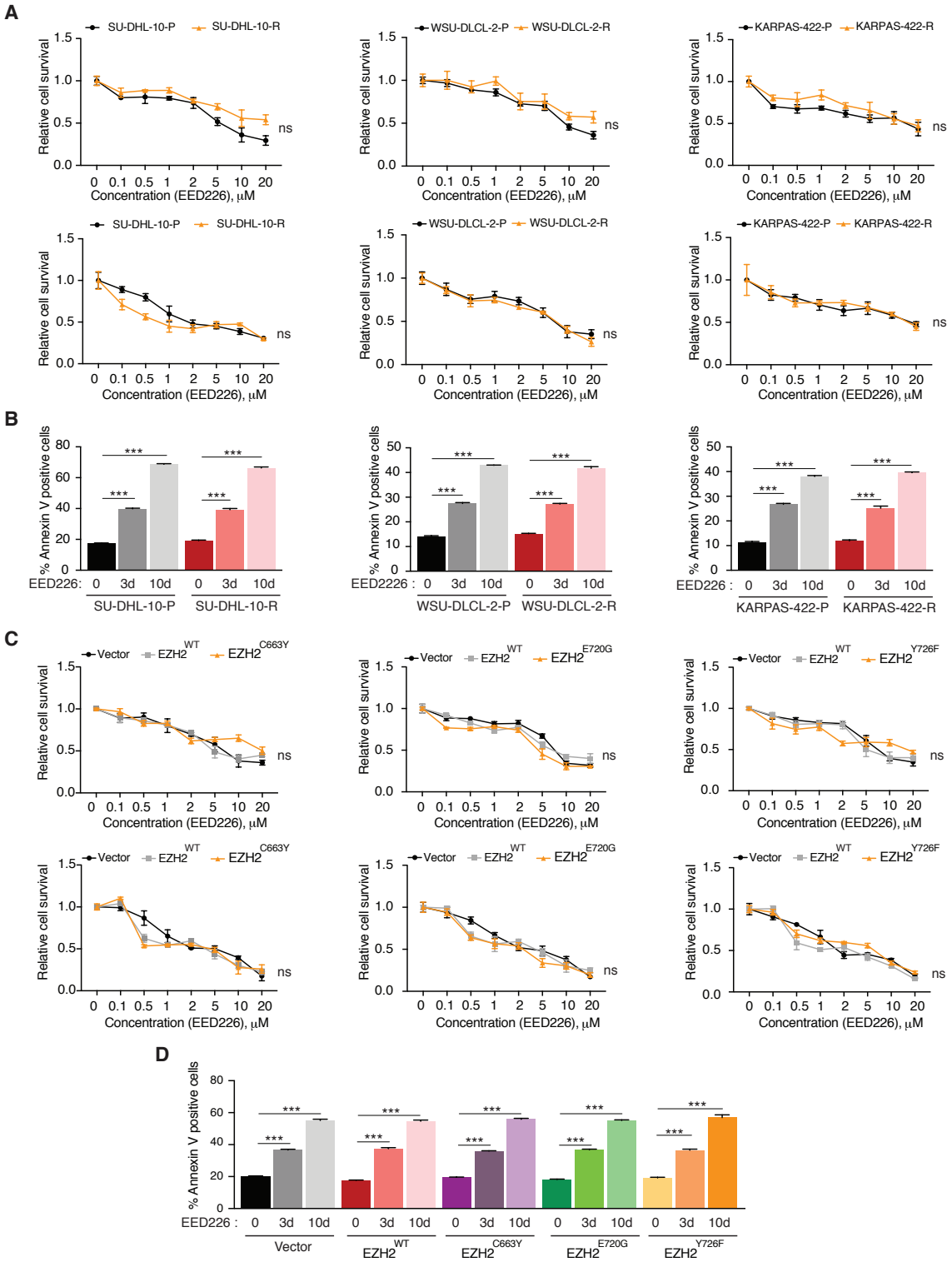

Figure S10. EZH2^{C663Y} and EZH2^{Y726F} mutants remained sensitive to the EZH2 inhibitor EED226. (A) Parental and GSK126-resistant DLBCL cells were treated with the indicated concentration of EED226 for 3 days (Top) or 10 days (Bottom) and assayed for cell viability by MTT. The cell viability relative to untreated cells is shown. (B) Parental and GSK126-resistant DLBCL cells were treated with EED226 (5 μM) for 3 or 10 days and apoptosis was analyzed by annexin V-FITC staining. (C) SU-DHL-10 cells overexpressing EZH2^{WT}, EZH2^{C663Y}, EZH2^{E720G}, EZH2^{Y726F}, or empty vector were treated with the specified concentrations of EED226 for 3 days (Top) or 10 days (Bottom) and assayed for cell viability by MTT. The cell viability relative to untreated cells is shown. (D) SU-DHL-10 cells overexpressing either EZH2^{WT}, EZH2^{C663Y}, EZH2^{E720G}, EZH2^{Y726F}, or an empty vector were treated with EED226 (5 μM) for 3 or 10 days and apoptosis was analyzed by annexin V-FITC staining. An area

under the curve (AUC) was calculated to allow for the comparison between the two curves and the p-values were calculated using a t-test. Data are presented as mean ±SEM; ns=not significant, *** = $p<0.001$.

Table S1. Ingenuity pathway analysis of altered genes from DLBCL cells (SU-DHL-10, KARPAS-422, WSU-DLCL-2, SU-DHL-6, DB, PFEIFFER and OCI-Ly-19) treated with a highly-selective small molecule inhibitor of EZH2, GSK126 (500 nM) for 72 h.

Categories	Diseases or Functions Annotation	p-Value	Molecules	# Molecules
Cancer, Cell Death and Survival, Organismal Injury and Abnormalities	apoptosis of head and neck tumor	1.75E-04	TGFBR1,TNFSF10	2
Cancer, Cell Death and Survival, Organismal Injury and Abnormalities	apoptosis of squamous-cell carcinoma	1.75E-04	TGFBR1,TNFSF10	2
Cell Death and Survival	cell viability of hepatoma cell lines	2.23E-04	CLU,PACS2,TBC1D9,TNFSF10	4
Cell Death and Survival	cell death of ovarian cancer cell lines	9.65E-04	BAD,CLU,FOXO3,MAPK8,SLC3A2,TNFSF10	6
Cell Death and Survival	apoptosis of rhombencephalon	1.13E-03	BAD,HDAC4,MAPK8	3
Cell Death and Survival, Skeletal and Muscular System Development and Function	cell viability of muscle cells	1.40E-03	APLN,FBXO32,FOXO3,MAPK8	4
Cancer, Cell Death and Survival, Organismal Injury and Abnormalities, Tumor Morphology	apoptosis of melanoma cells	1.70E-03	BAD,MAGEH1,TNFSF10	3
Cell Death and Survival, Gastrointestinal Disease, Hepatic System Disease, Organismal Injury and Abnormalities	apoptosis of liver cell lines	1.87E-03	BAD,FOXO3,TNFSF10	3
Cancer, Cell Death and Survival, Organismal Injury and Abnormalities, Tumor Morphology	apoptosis of mammary tumor cells	2.04E-03	BAD,TNFSF10,TPM1	3
Cell Death and Survival	apoptosis of connective tissue cells	2.45E-03	APLN,BAD,CLU,E2F2,FOXO3,MAPK8,PDGFB,TGFBR1,TNFSF10	9
Cell Death and Survival	cell death of brain	2.45E-03	BAD,CLU,FOXO3,GCLM,HDAC4,INPP4A,KCNJ6,MAPK8,TNFSF10	9
Cell Death and Survival	apoptosis of hepatoma cell lines	2.62E-03	BAD,CLU,FOXO3,MAPK8,PACS2,TNFSF10	6
Cell Death and Survival	apoptosis of osteoblasts	2.63E-03	APLN,BAD,TNFSF10	3
Cell Death and Survival	apoptosis of brain	2.77E-03	BAD,FOXO3,GCLM,HDAC4,KCNJ6,MAPK8	6
Cell Death and Survival	apoptosis of breast cell lines	3.06E-03	BAD,FOXO3,TGFBR1,TNFSF10	4
Cell Death and Survival	apoptosis of neuroblastoma cell lines	3.65E-03	CLU,FOXO3,MAPK8,PRKCB,TNFSF10	5
Cell Death and Survival	apoptosis of bone cell lines	3.67E-03	BAD,MAPK8	2
Cell Death and Survival	cell death of fibroblasts	3.83E-03	BAD,CLU,E2F2,FOXO3,LMNA,MAPK8,PDGFB,TNFSF10	8
Cell Death and Survival	apoptosis of central nervous system cells	4.10E-03	BAD,FOXO3,GCLM,HDAC4,KCNJ6,TNFSF10	6
Cell Death and Survival, Neurological Disease, Organismal Injury and Abnormalities	cell death of granule cells	4.17E-03	BAD,FOXO3,HDAC4,KCNJ6	4
Cell Death and Survival	cell viability of mesothelioma cell lines	5.01E-03	MAPK8,TNFSF10	2
Cell Death and Survival	apoptosis of skin cell lines	5.75E-03	MAPK8,TNFSF10	2
Cell Death and Survival	apoptosis of stomach cancer cell lines	6.67E-03	PRKCB,RTKN,TNFSF10	3

Cell Death and Survival, Organismal Injury and Abnormalities	cell death of epithelial cell lines	6.97E-03	BAD,FOXO3,HUS1B,IL17RD,MAPK8,PRKCB,TGFBR1,TNFSF10	8
Cell Death and Survival	cell death of breast cancer cell lines	7.65E-03	BAD,CLU,FBXO32,FOXO3,HDAC4,MAPK8,RTKN,TGFBR1,TNFSF10	9
Cardiovascular Disease, Cell Death and Survival, Connective Tissue Disorders, Hematological Disease, Hereditary Disorder, Organismal Injury and Abnormalities	amorph type Rh-null disease	7.67E-03	RHCE/RHD	1
Cancer, Cell Death and Survival, Organismal Injury and Abnormalities, Tumor Morphology	anoikis of mammary tumor cells	7.67E-03	TPM1	1
Cell Death and Survival	antiapoptosis of neuroblastoma cell lines	7.67E-03	PDGFB	1
Cell Death and Survival	apoptosis of progenitor-derived astrocytes	7.67E-03	TNFSF10	1
Cardiovascular System Development and Function, Cell Death and Survival, Skeletal and Muscular System Development and Function	cell survival of cardiomyocytes	7.67E-03	FBXO32	1
Cell Death and Survival, Cellular Function and Maintenance	colony survival of neuroblastoma cell lines	7.67E-03	TNFSF10	1
Cell Death and Survival, Free Radical Scavenging	cytotoxicity of superoxide	7.67E-03	CLU	1
Cell Death and Survival	killing of melanocytes	7.67E-03	TNFSF10	1
Cell Death and Survival	quantity of apoptotic endothelial cell lines	7.67E-03	TNFSF10	1
Cell Death and Survival, Reproductive System Development and Function	survival of oocytes	7.67E-03	KCNJ6	1
Cell Death and Survival, Cellular Compromise	toxicity of cerebellar granule cell	7.67E-03	GCLM	1
Cell Death and Survival, Gastrointestinal Disease, Hepatic System Disease, Organismal Injury and Abnormalities	necrosis of liver	7.72E-03	ABCB4,BAD,FOXO3,MAPK8,PDGFB,SLC25A4,TNFSF10	7
Cardiovascular Disease, Cell Death and Survival, Organismal Injury and Abnormalities	myocardial necrosis	7.84E-03	GABRA3,GABRB1,THBS4	3
Cell Death and Survival, Neurological Disease, Organismal Injury and Abnormalities	apoptosis of granule cells	8.26E-03	BAD,HDAC4,KCNJ6	3
Cell Death and Survival	apoptosis of breast cancer cell lines	8.66E-03	BAD,CLU,FBXO32,FOXO3,HDAC4,MAPK8,TGFBR1,TNFSF10	8
Cell Death and Survival	apoptosis of skin cancer cell lines	9.18E-03	CLU,TNFSF10	2
Cell Death and Survival	cell death of neuroblastoma cell lines	9.49E-03	BAD,CLU,FOXO3,MAPK8,PRKCB,TNFSF10	6
Cell Death and Survival, Gastrointestinal Disease, Hepatic System Disease, Organismal Injury and Abnormalities	cell death of liver cells	1.01E-02	BAD,FOXO3,MAPK8,PDGFB,SLC25A4,TNFSF10	6

Cell Death and Survival, Neurological Disease, Organismal Injury and Abnormalities	apoptosis of brain cells	1.06E-02	BAD,FOXO3,GCLM,HDAC4,KCNJ6	5
Cell Death and Survival	apoptosis of bone cancer cell lines	1.11E-02	CLU,FOXO3,MAPK8,PRKCB,TNFSF10	5
Cell Death and Survival, Neurological Disease, Organismal Injury and Abnormalities	apoptosis of cerebellar granule cell	1.12E-02	BAD,HDAC4	2
Cell Death and Survival	apoptosis of hepatic stellate cells	1.12E-02	PDGFB,TNFSF10	2
Cell Death and Survival, Organismal Injury and Abnormalities	apoptosis of vascular endothelial cells	1.13E-02	FOXO3,MAPK8,TGFBR1,TNFSF10	4
Cancer, Cell Death and Survival, Organismal Injury and Abnormalities, Tumor Morphology	apoptosis of neuroblastoma cells	1.22E-02	CLU,TNFSF10	2
Cell Death and Survival	apoptosis of fibroblast-like synoviocytes	1.33E-02	CLU,TNFSF10	2
Cell Death and Survival	apoptosis of rhabdomyosarcoma cell lines	1.33E-02	PRKCB,TNFSF10	2
Cell Death and Survival, Skeletal and Muscular Disorders	apoptosis of muscle cell lines	1.37E-02	BAD,LMNA,TNFSF10	3
Cell Death and Survival	apoptosis of MCTC mast cell	1.53E-02	FOXO3	1
Cell Death and Survival	apoptosis of articular chondrocytes	1.53E-02	TNFSF10	1
Cancer, Cell Death and Survival, Organismal Injury and Abnormalities, Tumor Morphology	apoptosis of cholangiocarcinoma cell	1.53E-02	TNFSF10	1
Cell Death and Survival	apoptosis of duct cancer cell lines	1.53E-02	TNFSF10	1
Cancer, Cell Death and Survival, Organismal Injury and Abnormalities, Tumor Morphology	apoptosis of leukemic blasts	1.53E-02	TNFSF10	1
Cell Death and Survival	apoptosis of mucosal mast cells	1.53E-02	FOXO3	1
Cell Death and Survival	arrest in apoptosis of carcinoma cell lines	1.53E-02	TNFSF10	1
Cell Death and Survival	arrest in apoptosis of lung cancer cell lines	1.53E-02	TNFSF10	1
Cell Death and Survival, Cellular Function and Maintenance	clearance of Streptococcus pneumoniae strain EF3030	1.53E-02	TNFSF10	1
Cell Death and Survival, Cellular Compromise	cytotoxicity of lung cancer cell lines	1.53E-02	TNFSF10	1
Cell Death and Survival, Cellular Compromise	cytotoxicity of lymphoblasts	1.53E-02	TNFSF10	1
Cell Death and Survival	delay in cell death of cervical cancer cell lines	1.53E-02	TNFSF10	1

Table S2: Primer sequences for RT-qPCR analysis; clone ID and catalog numbers for shRNAs (Open Biosystems); antibodies used; source and concentration of chemical inhibitors used.

Application	**Gene symbol**	**Forward primer (5′-3′)**	**Reverse primer (5′-3′)**
RT-qPCR	ABCA1	AGCTGAGGTTGCTGCTGTGG	CCCCTGAACCCAAGGAAGTG
	SEPT8	GGTGAAGGTGGGGAACAAGC	GCGCCGGTAGAGCTCGTAGT
	ABAT	GCTGAGAGACATCGCCAGGA	TCATCACGTCTGCTGGGTCA
	SERPINB6	ACGAGGCTGGACATGATGGA	TGTGCACGACCTTGGACAGA
	CNR1	ATCGGGGTCACCAGCGTACT	GCCGGGTCACCTGTACCTTC
	RBM9	CTGCTGCATTTCCAGGGATG	TCAAAAGGTGACGGGGAGGT
	SESN1	ACCCCAAGTGGCTCAATGGT	GGGACCAGCTGTGCTCTTCA
	MSRB2	TGGCAAAGCAGGAGCAAGAG	TCATGGCTTGGTGCTGTCCT
	ELK3	TCTTCACCGCACAGACACCA	CAGACTGGGGATTGGCACTG
	SESN3	CGAGGCTTCCTCAGGTGGAT	AGGCTATGCCCCAGATTCCA
	APLN	CCCAGGGTGGTTTTCAGGAG	CCTTCTGCCCTTCCCTTCCT
	FOSB1	GGGGTGACAGTCCTCCATCC	CAAGGGGTGGGAGAAGTTGG
	BEX2	CGAGAATCGGGAGGAGGAGA	CCTCTGCAGGCACCAAAATG
	SPINK1	ACCTGGAGGGCCAGCTATGA	GAGTTCCGCGTCAGAGGTCA
	EGR2	TGGGCATAAGCCCTTCCAGT	GGCACTGCTTTTCCGCTCTT
	BEND5	CCCTCGCAGAGGGAGACATT	TTGGAGGAGCCCCCATAGAA
	BIRC3	AGCAATTGGGAACCGAAGGA	TTAAAGCGGGCTGCATGTGT
	EZH2	TCCCGCTGAGGATGTGGATA	GGGCACGAACTGTCACAAGG
	BAD	TCCTGGTGGGATCGGAACTT	CGGAAGGGAATCTGGGTCAG
	TNFSF10	AGCTGGGTGTGTTGGCACAT	CGCCAGGCTGGAGTGTAGTG
	FOXO3	CATGGACGACCTGCTGGATA	CCGAACACCGTGCTGTTAAA
EZH2 mutation screening	**Exon**	**Forward primer (5′-3′)**	**Reverse primer (5′-3′)**
	15	TCCATTAATTGACTTTTCCAGTG	ACCTCCACCAAAGTGCAAAG
	16	ACCTCCACCAAAGTGCAAAG	TTCTCTTCCATCAAAATGAGTTTTAG
	17	TTCTCTTCCATCAAAATGAGTTTTAG	TCCTCACAACACGAACTTTCAC
	18	TCCTCACAACACGAACTTTCAC	GAGTTGTCCTCATCTTTTCGC
	19	GAGTTGTCCTCATCTTTTCGC	CCAAGAATTTTCTTTGTTTGGAC
	20	CCAAGAATTTTCTTTGTTTGGAC	AAGAATGGTTTGCCTAAATAAGAC
TA Amplification	**Name**	**Forward primer**	**Reverse primer**
	TA	GGGGATGTGCTGCAAGGCGA	TGAGTTAGCTCACTCATTAG
Sequencing	**Name**	**Forward primer**	**Reverse primer**
	Sp6		ATTTAGGTGACACTATAG
	M13	GTAAAACGACGGCCAG	CAGGAAACAGCTATGAC
Site directed mutagenesis	**Mutation**	**Forward primer (5′-3′)**	**Reverse primer (5′-3′)**
	Y641F	*CATCTCAGAATTCTGTGGAGAGA*	*TCTCTCCACAGAATTCTGAGATG*
	C663Y	GTGTATGATAAATACATG**TAC**AGCTTTC TGTTCAACTTG	CAAGTTGAACAGAAAGCT**GTA**CATGT ATTTATCATACAC
	E720G	AGCCATCCAGACTGGC**GGA**GAGCTGTT TTTTGAT	ATCAAAAAACAGCTC**TCC**GCCAGTCT GGATGGCT
	Y726F	GCGAAGAGCTGTTTTTTGAT**TTC**AGATA CAGCCAGGC	GCCTGGCTGTATCT**GAA**ATCAAAAAA CAGCTCTTCGC
shRNAs	**Gene symbol**	**Clone ID**	**Catalog number**
	TNFSF10	RHS3979-9574773	TRCN0000005925
	TNFSF10	RHS3979-9574774	TRCN0000005926
	BAD	RHS3979-9600864	TRCN0000033456
	BAD	RHS3979-9600865	TRCN0000033457
	FOXO3A	RHS3979-9607487	TRCN0000040098
	FOXO3A	RHS3979-9607489	TRCN0000040100
Immunoblotting	**Protein symbol**	**Antibody source**	**Dilution**
	EZH2	Cell signaling	1:1000
	Cyclin D1	BD Bioscience	1:500
	Phospho-IGF-1R	Cell signaling	1:1000
	Total-IGF-1R	Cell signaling	1:1000

	Phospho -AKT	Cell signaling	1:1000
	Total-AKT	Cell signaling	1:1000
	Phospho-ERK	Cell signaling	1:1000
	Total-ERK	Cell signaling	1:1000
	MEK1/2	Cell signaling	1:1000
	H3K27me3	Cell signaling	1:2000
	Histone 3	Cell signaling	1:2000
	LC3-B	Cell signaling	1:1000
	P62	Cell signaling	1:1000
	Phospho-FOXO3	Cell signaling	1:1000
	Total-FOXO3	Cell signaling	1:1000
	BAD	Cell signaling	1:1000
	TNFSF10	Cell signaling	1:1000
	ACTINB	Cell signaling	1:2500
Pharmacological agents	**Compounds**	**Concentration**	**Source**
	GSK126	Indicated concentrations	MedChem Express
	EPZ-6438	Indicated concentrations	MedChem Express
	UNC1999	Indicated concentrations	SelleckChem
	EED226	Indicated concentrations	MedChem Express
	Pictilisib (GDC-0941)	Indicated concentrations	SelleckChem
	Linsitinib (OSI-906)	Indicated concentrations	SelleckChem
	Trametinib (GSK1120212)	Indicated concentrations	SelleckChem
	Ethyl methanesulfonate (EMS)	2 mM	Sigma-Aldrich
	Rapamycin	500 nM	Enzo Life Sciences
	Chloroquin	10 μM	Enzo Life Sciences